Endosidin1 defines a compartment involved in endocytosis of the brassinosteroid receptor BRI1 and the auxin transporters PIN2 and AUX1

Stéphanie Robert, S. Narasimha Chary, Georgia Drakakaki, Shundai Li*, Zhenbiao Yang, Natasha V. Raikhel, and Glenn R. Hicks†

Center for Plant Cell Biology, Institute for Integrative Genome Biology and Department of Botany and Plant Sciences, University of California, Riverside, CA 92521

Edited by Joanne Chory, Salk Institute for Biological Studies, La Jolla, CA, and approved April 1, 2008 (received for review December 10, 2007)

Although it is known that proteins are delivered to and recycled from the plasma membrane (PM) via endosomes, the nature of the compartments and pathways responsible for cargo and vesicle sorting and cellular signaling is poorly understood. To define and dissect specific recycling pathways, chemical effectors of proteins involved in vesicle trafficking, especially through endosomes, would be invaluable. Thus, we identified chemicals affecting essential steps in PM/endosome trafficking, using the intensely localized PM transport at the tips of germinating pollen tubes. The basic mechanisms of this localized growth are likely similar to those of non-tip growing cells in seedlings. The compound endosidin 1 (ES1) interfered selectively with endocytosis in seedlings, providing a unique tool to dissect recycling pathways. ES1 treatment induced the rapid agglomeration of the auxin translocators PIN2 and AUX1 and the brassinosteroid receptor BRI1 into distinct endomembrane compartments termed ''endosidin bodies''; however, the markers PIN1, PIN7, and other PM proteins were unaffected. Endosidin bodies were defined by the syntaxin SYP61 and the V-ATPase subunit VHA-a1, two *trans*-Golgi network (TGN)/endosomal proteins. Interestingly, brassinosteroid (BR)-induced gene expression was inhibited by ES1 and treated seedlings displayed a brassinolide (BL)-insensitive phenotype similar to a *bri1* loss-of-function mutant. No effect was detected in auxin signaling. Thus, PIN2, AUX1, and BRI1 use interactive pathways involving an early SYP61/VHA-a1 endosomal compartment.

endosome | *Arabidopsis* | chemical genomics | prieurianin

Diverse organisms including plants display unidirectional cellular growth. This is true of many cell types, but it is especially obvious in root hairs and pollen tubes and requires calcium gradients, cytoskeleton, and tip-focused vesicle trafficking (1), which are coordinated via ROPs (Rho-related GTPases) (2–4). The maintenance of polarized growth requires ROP-interacting proteins, such as ICR1 (2). This complex apparatus has evolved to direct the delivery of newly synthesized proteins toward the site of growth and to modulate their internalization at the PM (endocytosis). Related but less specialized processes are present in cells displaying less polarized growth, such as in roots. Although proteins travel through intermediate compartments (endosomes) when transiting to or from the PM (5, 6), their nature and the mechanisms by which their cargoes are recycled to the PM (7) or sorted to late endosomes and the prevacuolar compartment (PVC) for degradation in the vacuole are poorly understood (8). There is evidence in plants that the TGN functions as an early endosome compartment (9), adding to the complexity of endosome sorting mechanisms. Sorting occurs in a TGN/early endosome network from which proteins are trafficked to later endosomes marked by GNOM, a GDP-GTP exchange factor for ARF GTPases (ARF-GEF) or SORTING NEXIN1 (AtSNX1) (10–12). Again, sorting results ultimately in either recycling to the PM or turnover. In addition to transport, endosomes serve a role in signaling in eukaryotes (13, 14). An example in plants is BRI1, a leucine-rich repeat kinase receptor (LRR) that is found at the PM and endosomes and recognizes brassinosteroids (BRs). These hydroxylated steroids regulate plant growth and development (15). Recent evidence indicates that, in *Arabidopsis thaliana*, the endosomal pool of BRI1 is critical for signaling and regulation of BR-responsive genes (16). Additional studies of ARF-GEFs (17, 18), including GNOM (19) and sterol trafficking (20), demonstrate the necessity of endocytosis and endosome sorting for development. Given the highly dynamic nature of endomembrane trafficking and its essentiality we reasoned that specific fast-acting chemical modulators would deepen our understanding of endocytosis, endosomal sorting, and recycling. A paradigm for such reagents is Brefeldin A (BFA), which has yielded knowledge of ARF-GEF-dependent pathways (17, 18). Thus, we screened for chemicals that affected sorting processes. One chemical, endosidin 1 (ES1), blocked the endocytosis of several PM auxin transporters, which are known to recycle in *Arabidopsis* roots. These transporters traffic through a TGN/endosome compartment containing the proteins SYP61 and VHA-a1. The BRI1 receptor also trafficked through this SYP61/VHA-a1 endosomal compartment, indicating that at least three PM proteins share overlapping endocytic pathways.

Results and Discussion

We developed an automated image-based screen for compounds that inhibited pollen germination *in vitro* or affected polar growth (pollen tube tip swelling), which depend on vesicle transport [supporting information (SI) Fig. S1 *a–e*]. A subset of these inhibitors caused the mis-localization of a tip-localized marker associated with the PM, a GFP fusion to the *Arabidopsis* ROP interacting partner 1 (GFP-RIP1) (At1g17140). GFP-RIP1, recently published as ICR1 (2), localized to the apical PM of *Arabidopsis* and tobacco pollen tubes (Fig. S1 *a* and *f–i*). From a screen of 2,016 chemicals, we obtained several that caused mislocalization of GFP-RIP1 and resulted in increased cytosolic localization of GFP-RIP1, inappropriate localization at the tip, and loss of polar growth (Fig. S1 *j–m*). One compound was the PP2A phosphatase inhibitor cantheridin. A PP2A was recently demonstrated to be involved in apical/basal PM localization of

Author contributions: S.R., S.N.C., G.D., and G.R.H. designed research; S.R., S.N.C., G.D., S.L., and G.R.H. performed research; S.R., S.N.C., G.D., S.L., Z.Y., and G.R.H. contributed new reagents/analytic tools; S.R., N.V.R., and G.R.H. analyzed data; and S.R. and G.R.H. wrote the paper.

The authors declare no conflict of interest.

This article is a PNAS Direct Submission.

*Present address: Department of Plant Biology, Carnegie Institution of Washington, Stanford University, 260 Panama Street, Stanford, CA 94305.

†To whom correspondence should be addressed. E-mail: ghicks@ucr.edu.

This article contains supporting information online at www.pnas.org/cgi/content/full/0711650105/DCSupplemental.

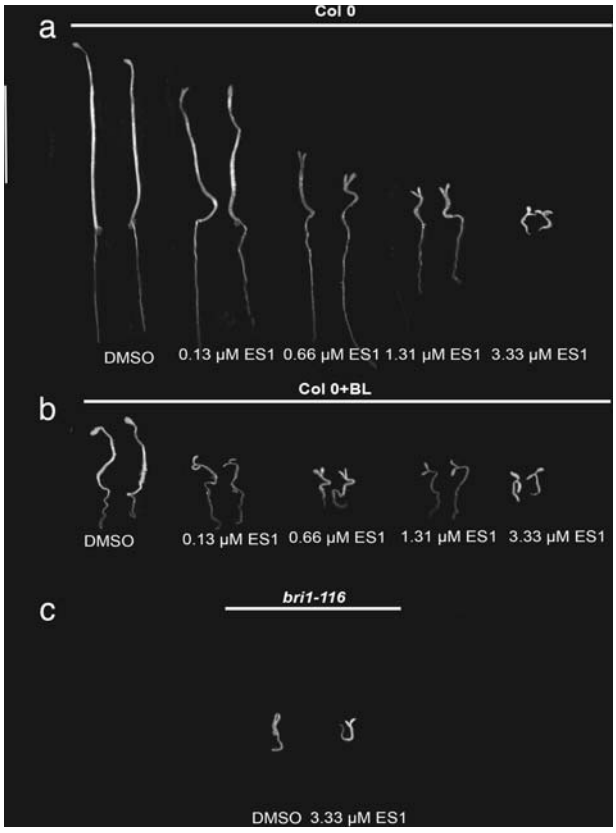

Fig. 1. ES1 phenocopies a mutant defective in BR signaling. (*a*) Ten-day-old wild-type (Col-0) seedlings grown in the dark in the absence (DMSO) or presence of the indicated concentrations of ES1. ES1-treated seedlings displayed shorter bent hypocotyls and open expanded cotyledons similar to the phenotype of the receptor mutant *bri1-116* (*c*). (*b*) When seedlings were grown in the presence of 1 μM BL and no ES1 (DMSO) or BL plus increasing concentrations of ES1 as indicated, the BL-induced phenotype was not relieved by ES1, indicating no effect on BL biosynthesis. (*c*) The BL-insensitive mutant *bri1-116* was unaffected by ES1. (Scale bar, 1 cm.)

PIN auxin transporters (21); thus, the identification of cantheridin as affecting RIP-GFP localization provided validation our screening approach. Another compound that was active in our assay in the low micromolar range was reported as prieurianin, a limonoid displaying ecdysone antagonist and anti-feedant activity in insects (22, 23); however, we propose the name endosidin1 (ES1), which is descriptive of its cellular mode of action. Related limonoids were without effect indicating the selectivity of the screen for ES1 (Table S1). In addition to its potency, we focused on ES1 because it resulted in dramatic effects on seedlings at the whole plant and cellular levels.

Seedlings grown in the presence of ES1 displayed dose-dependent inhibition of hypocotyl and root development. However, when grown in the dark in the presence of ES1, seedlings had a light-grown phenotype that increased with concentration. The characteristics of the phenotype were increased hypocotyl thickening, increased cotyledon expansion and opening, and decreased straight growth habit, resulting in highly bent hypocotyls (Fig. 1*a*) similar to that of the brassinosteroid receptor mutant *bri1-116* (24) (Fig. 1*c*). Growth in the presence of 1 μM exogenous BL resulted in growth inhibition that was not relieved by ES1; at higher ES1 concentrations, the *bri1*-like phenotypes (cotelydon expansion and opening, bent hypocotyls) were enhanced (Fig. 1*b*). This additive effect suggested that ES1 did not antagonize BR biosynthesis or perception, which would have resulted in taller, more etiolated seedlings than the control. Overall, the seedling phenotypes suggested the possibility that one mode of action of ES1 may be to affect a pathway related to BR perception, signaling or response. Recently, BR signaling has been proposed to occur via endosomes (16), prompting us to ask whether ES1 affected the endomembrane system.

To determine whether ES1 affected endocytosis or recycling at the PM, we examined its impact on five well characterized marker proteins that recycle through endosomes in the root tips of *Arabidopsis* seedlings. They were the auxin transporters PIN1, PIN2, PIN7, and AUX1 and the BR receptor BRI1. When 4-day-old light-grown seedlings were exposed to 33 μM ES1 (and as little as 3.3 μM; data not shown) for 2 h to detect primary effects, PIN2-GFP (25), AUX1-YFP (26) and BRI1-GFP (16) formed intracellular agglomerations that we termed "endosidin bodies" (Fig. 2 *a–f*). Unlike pollen, a higher concentration of ES1 was necessary to see consistent effects on markers, which may be a reflection of cellular and morphological differences between single-celled pollen and multicellular root tissues. The markers PIN1-GFP (27) and PIN7-GFP (28) were unaffected (Fig. 2 *g–j*) even after 12 h (data not shown). Endosidin bodies marked by AUX1-YFP and BRI1-GFP were throughout the root tip (Fig. 2 *d* and *f*), demonstrating that ES1 penetrated all detectable cell layers. Our results indicated that ES1 selectively disrupted the trafficking of PIN2, AUX1, and BRI1 but not PIN1 and PIN7, suggesting at least two pathways for endocytosis or recycling. Consistent with these results, a previous study, using BFA, suggested that AUX1 and PIN1 are recycled via different pathways (29). Notably, the polar PM localization typically displayed by PIN2 in the epidermis and cortex did not appear to be affected by ES1 (Fig. 2 *a* and *b*). Thus, we concluded that ES1 did not interfere significantly with mechanisms of asymmetric localization at the root PM, which may have differences compared with pollen tube growth polarity. In support of this, ES1 did not induce an auxin-specific reporter (Fig. S2*b*) nor did it inhibit gravitropism, which depends on PIN asymmetry (30–32) (Fig. S2*a*). The effects of ES1 on PIN2-GFP were reversible (Fig. S3 *a* and *b*), as were the effects on seeding development (Fig. S3*c*).

To understand the specificity of ES1, we first examined endomembrane markers at 33 μM ES1. The PM marker PIP2A-GFP (33) (Fig. S4 *a* and *b*) was unaffected as were KDEL-GFP (34) (ER) (Fig. S4 *i* and *j*), SYP21- and SYP22-YFP (prevacuole compartment) (Fig. S4 *e* and *f*), MAN-YFP (35), and NAG1-GFP (20) (Golgi) (Fig. S4 *g* and *h*). We then focused on endosomal compartments, using the marker ARA7-GFP (36) (Fig. S4 *c* and *d*) and ARA6-GFP (6, 20, 36), BOR1-GFP (37), GFP-KOR (38), SNX1-GPF (36), GNOM-GFP (19), and the TGN marker TLG2a-GFP (SYP41) (36) (data not shown). In each case, no effect was observed.

Remarkably, when we examined SYP61-CFP, defined as TGN (39), intracellular bodies were apparent with ES1 in all visible cell layers of the root tip (Fig. 3*e*). The TGN marker, VHA-a1-GFP (9), colocalized with SYP61-CFP in the absence and presence of ES1 (Fig. S5 *a–f*), suggesting that both markers highlighted endosidin bodies. To confirm this, lines coexpressing PIN2-GFP and SYP61-CFP were examined. PIN2-GFP colocalized occasionally with SYP61-CFP (Fig. 3 *a–c*); however, with ES1, PIN2-GFP and SYP61-CFP colocalized frequently within the same endosidin bodies (Fig. 3 *d–f*). AUX1-YFP and BRI1-GFP displayed similar colocalization with SYP61-CFP in the presence ES1 (data not shown). Overall, ES1 disrupted a TGN/endosome compartment defined by SYP61 and VHA-a1 but not SYP41. Furthermore, this compartment resided within the same pathway of endocytosis or recycling as PIN2, AUX1, and BRI1.

To determine where ES1 was acting in endosome trafficking, we took advantage of the plant hormone auxin, which inhibits the early endocytosis of PINs and other PM proteins (40).

PLANT BIOLOGY

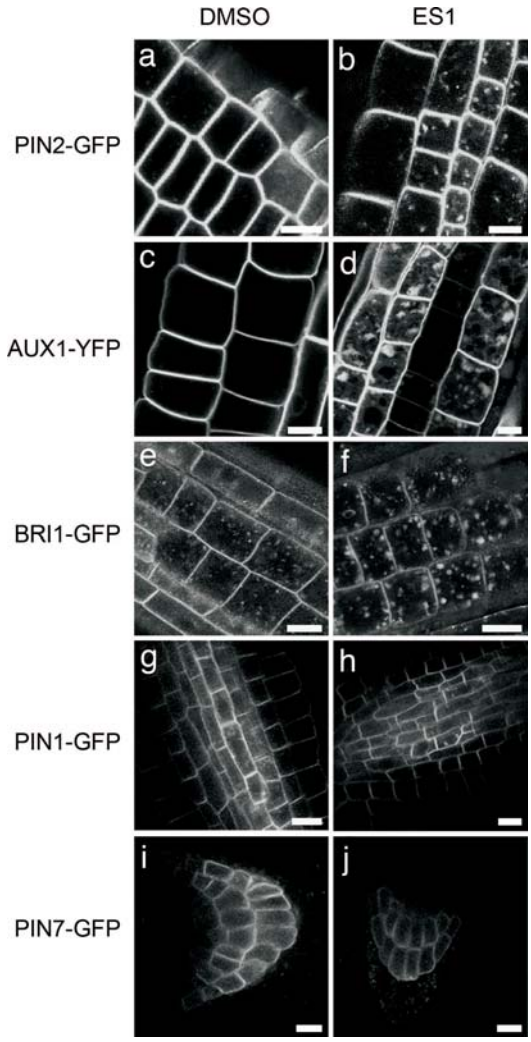

Fig. 2. ES1 induces intracellular bodies selectively. Four-day-old *Arabidopsis* seedlings expressing the indicated markers were treated for 2 h with DMSO only as a control (*a*, *c*, *e*, *g*, and *i*) or with 33 μM ES1 (*b*, *d*, *f*, *h*, and *j*). Compared with PIN2-GFP fluorescence in the control (*a*) intracellular bodies are apparent in cells after ES1 treatment (*b*). In *a* and *b*, the root apex is toward the bottom of the image, and the basal localization of PIN2-GFP is apparent. The asymmetric PM localization is visible in epidermal cells in the control and ES1-treated samples, indicating no qualitative effect of ES1 on this asymmetry. (*c* and *d*) AUX1-YFP fluorescence is visible at the PM, but in ES1-treated seedlings, intracellular bodies are apparent (*d*). (*e*) BRI1-GFP fluorescence shows the normal presence of BRI1-GFP at the PM and in endosomes. However, ES1 treatment (*f*) resulted in large intracellular bodies. Neither PIN1-GFP (*g* and *h*) nor PIN7-GFP (*I* and *j*) fluorescence indicated any effect of ES1. All images were generated by using a 63× objective. (Scale bars, 10 μm.)

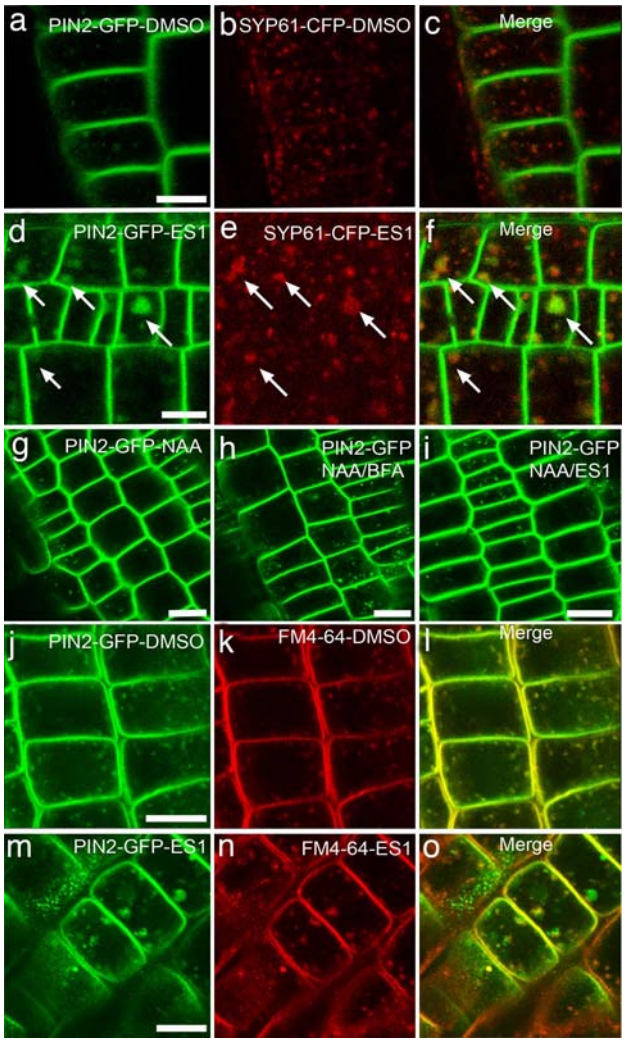

Fig. 3. ES1 impacts endocytosis and SYP61-containing endosomes. (*a–f*) Seedling roots coexpressing PIN2-GFP and SYP61-CFP. In controls (DMSO), PIN2-GFP (*a*) and SYP61-CFP (*b*) showed occasional colocalization in endosomes in merged images (*c*). However, in the presence of 33 μM ES1 for 2 h, endosidin bodies (arrows) were apparent with either PIN2-GFP (*d*) or SYP61-CFP (*e*). In merged images, PIN2-GFP and SYP61-CFP fluorescence signal showed close proximity and overlap especially at largest bodies (*f*), indicating that SYP61-CFP marks endosidin bodies (arrows). (*g–l*) Seedlings expressing PIN2-GFP were treated with 5 μM NAA for 30 min followed by addition of either 50 μM BFA or 33 μM ES1 and incubation for an additional 90 min. Among controls, NAA had no obvious effect on PIN2-GFP fluorescence (*g*); however, as reported in ref. 40, NAA blocked the formation of BFA bodies (*h*). NAA also blocked the formation of endosidin bodies, indicating that PIN2-GFP gained entry into bodies via endocytosis (*i*). (*j–o*) Seedlings expressing PIN2-GFP were treated with 4 μM of the endocytic dye FM4-64 and imaged within 5 min of dye addition. In controls (DMSO), PIN2-GFP (*j*) and FM4-64 (*k*) fluorescence were strongly colocalized at the PM and endosomes (*i*). As before, when treated with 33 μM ES1 for 2 h, PIN2-GFP formed endosidin bodies (*m*). Although PM staining appeared unaffected, FM4-64 formed similar agglomerations (*n*) that colocalized with endosidin bodies. All images were generated by using a 63× objective. (Scale bars, 10 μm.)

Naphthalene-1-acetic acid (NAA) at 5 μM blocked the formation of PIN2-GFP labeled BFA bodies as reported in ref. 40 (Fig. 3 *g* and *h*). Significantly, NAA also blocked the incorporation of PIN2-GFP into endosidin bodies (Fig. 3*i* and Fig. S6). However, SYP61-CFP still agglomerated (Fig. S6 *a–f*), indicating that NAA blocked neither endosidin body formation nor uptake of ES1. Thus, we concluded that PIN2-GFP entry into endosidin bodies was via endocytosis, and ES1 acted on endocytosis after an earlier step blocked by NAA. Consistent with the NAA findings, ES1 did not block accumulation of the endocytic styryl dye FM4-64 into endosomal compartments or endosidin bodies (Fig. 3 *m–o*), which were visible within 5 min of dye addition (Fig. 3 *j–l*). Inhibition of protein synthesis by cycloheximide (41) did not prevent PIN2-GFP endosidin body formation indicating that entry was independent of protein synthesis and the delivery of newly synthesized proteins to the PM (data not shown). We concluded that ES1 affected the endocytosis and sorting of PIN2, AUX1, and BRI1 by impacting a pool of early endosomes defined by SYP61 and VHA-a1.

Endosomes are thought to be a site of intracellular BR signaling, and there is evidence that the BRI1 receptor in an

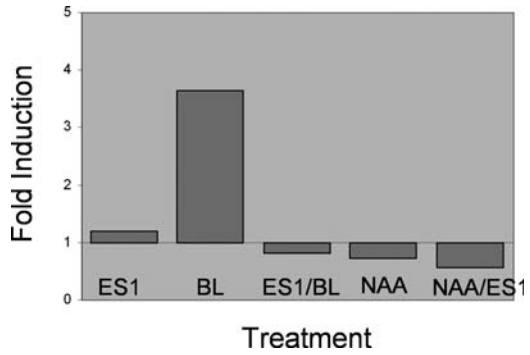

Fig. 4. ES1 inhibited the induction of a BL reporter gene. Quantitative PCR was used to detect the expression of a BL-specific NAC family transcription factor. Four-day-old seedlings were treated with 33 μM ES1, 1 μM BL, 5 μM NAA, or the combinations indicated for 3 h before RNA purification. PCRs were normalized by using unbiquitin. After PCR, ratios representing relative fold-induction were calculated (46). As controls, treatment with BL resulted in 3- to 4-fold induction (BL bar), whereas NAA (NAA bar) resulted in no induction, indicating the specificity for BL. Treatment with ES1 alone (ES1 bar) resulted in no induction. Significantly, ES1 plus BL (ES1/BL bar) resulted in no induction, indicating that ES1 inhibited BL signaling. NAA plus ES1 was without effect (NAA/ES1 bar). Data points are the mean of triplicates, and similar results were obtained in three independent experiments.

endosomal compartment is an essential participant (16). To determine whether endosidin impacted BR signaling, we examined the output of a BL-specific NAC family transcription factor (At5g46590) (42), using quantitative PCR (Fig. 4). After 3 h of treatment with 33 μM ES1 only, there was no induction indicating that ES1 was not an agonist of BR signaling. BR and auxin responses overlap; however, as reported in ref. 42, NAA treatment did not alter NAC gene expression indicating specificity for BL. Treatment with 1 μM BL resulted in a three- to fourfold induction of the NAC transcript. However, in the presence of ES1, reporter induction was inhibited significantly (Fig. 4), indicating that ES1 antagonized BR-signaling. Because an endosomal compartment containing BRI1-GFP was impacted by ES1, it raised the potential that ES1 interfered with BRI1 signaling from a SYP61/VHA-a1 endosomal compartment or with the trafficking of BRI1 to a downstream compartment where it was active in signaling. However, our data, although suggestive, does not conclusively establish that the formation of endosidin bodies is causal to defects in BR signaling. In addition, our data showing the cellular effects of ES1 may represent one of several modes of action. It is possible, for example, that the ES1's impacts on seedling morphology at lower concentrations and longer time periods could be due to a different mode of action such as effects on BR perception, especially given ES1's reported activity as an ecdysone antagonist (23). Thus, our data do not exclude the possibility that ES1 could display effects beyond of its action on endocytosis.

Our results highlight the complexity of endosomal sorting mechanisms and indicate the utility of bioactive chemicals for the dissection of highly dynamic endomembrane processes that might otherwise be inaccessible via genetics alone because of long-term compensatory mechanisms or gene redundancy. ES1 phenocopied a *bri1* mutant, and at least one of its modes of action is to block endocytosis at an early endosome compartment. Perturbing this endosome population, which did not affect the trafficking of PIN1 or PIN7, allowed us to recognize at least two pathways of endocytosis and sorting and to define one pathway that was used by PIN2, AUX1 and BRI1. The PIN2/AUX1/BRI1 pathway includes an early endosomal compartment defined by SYP61/VHA-a1 that marks endosidin bodies (Fig. S7).

Recently, Geldner *et al.* (16) reported that BRI1-GFP cycled constitutively between the PM and endosomes in *Arabidopsis* roots irrespective of BR. In the presence of BFA, agglomeration of BRI1-GFP-containing endosomes and other compartments, such as the Golgi, resulted in enhanced signaling presumably via an increase in a pool of endosomal BRI1. ES1 appears to display more compartment specificity in its action than BFA. For example, endosidin bodies do not sequester Golgi-specific markers or endosome markers other than SYP61 and VHA-a1.

An interesting aspect of ES1 is that, although it impacts polar growth of pollen tubes and the endocytosis of PIN2 and AUX1 in roots, it does not impact asymmetric PM localization and dependent responses such as gravitropism. This demonstrates that endocytosis and PM apical/basal localization mechanisms may be uncoupled by ES1. Jaillais *et al.* (11) reported recently that the retromer complex protein VPS29 may be involved in retrograde trafficking from a SNX1 compartment to the PVC and in initiating cell polarity and for maintaining endosome integrity. Among other features, SNX1 compartments may be late endosomes that function in the trafficking of PIN2 through the PVC (10). When examined in a *vps29* mutant background, SNX1-GFP compartments display an aberrant morphology (11). An important conclusion is that PIN1 is internalized through a BFA-sensitive GNOM endosomal compartment and then sorted to a SNX1 late compartment, where it is hypothesized that cargoes are sorted to the vacuole or recycled to the PM. Thus, GNOM endosomes proceed SNX1 late endosomes within the endocytic pathway of PIN1 (reviewed in ref. 12).

Only PIN2 endocytosis is affected by ES1; PIN1 is unaffected. Likewise, ES1 had no effect on GNOM endosomal compartments indicating that the chemical does not impact the PIN1 endocytic pathway. Rather, it impacts a pathway shared by PIN2, AUX1, and BRI1. No effect on the morphology of SNX1-GFP was observed in the presence of ES1, although it has been reported that PIN2 (like PIN1) is transported through SNX1 late endosomes and PVC (36). We have found that ES1 has no effect on the morphology of the PVC. Thus, the ES1-sensitive SYP61/VHA-a1 endosomal compartment precedes SNX1 compartments functionally (Fig. S7), which further supports the conclusion that SYP61/VHA-a1 defines an early endosomal compartment.

BRI1-GFP colocalizes with SNX1-mRFP (10), indicating that it traffics through both the SYP61/VHA-a1 early endosomal compartment and SNX1 late endosomes. Interestingly, PIP2A and BOR1 also traffic through SNX1 endosomes, whereas they are unaffected by ES1. Thus, in *Arabidopsis* roots the early endocytosis of PIN2, AUX1, and BRI1 use a SYP61/VHA-a1 ES1-sensitive endosomal compartment not shared with PIN1, PIN7, and BOR1, whereas such PM proteins likely share common steps in late endosomes or PVC (10).

Overall, the identification of SYP61/VHA-a1 as an early endosome compartment highlights the power of bioactive chemicals to dissect essential endomembrane processes. Additional reagents used either directly or via their molecular targets will allow us to dissect endocytic, recycling, and degradation pathways in greater detail.

Materials and Methods

Screen for Bioactive Chemicals. The chemical library (Microsource Spectrum) contained 2,016 chemicals with known biological activity (for contents, see www.msdiscovery.com). Chemical stocks were in 100% DMSO (10–20 mM) at the University of California, Riverside Center for Plant Cell Biology and arrayed in 384-well plates. Chemicals were distributed to 96-well clear-bottom plates (Nalge Nunc), using a Precision 2000 fluid robot (Bio-Tek). For the primary screen, pollen from wild-type tobacco (Samsun) was harvested at dehiscence. Anthers (150) from 30 flowers were suspended in 17 ml of GM2 medium [18% sucrose, 0.01% boric acid, 5 μM $CaCl_2$, 5 μM $Ca(NO_3)_2$, and 1 mM $MgSO_4$ (pH 6.5–7.0)] and vortexed to release pollen, then centrifuged at 50$\times$ for 1 min. Forty microliters of supernatant containing pollen was added to each well of

the screening plates. The final concentration of chemicals was 50–100 μM; the DMSO never exceeded 0.5%. Plates were incubated at room temperature on an orbital shaker at 70 rpm for a minimum of 3 h to permit germination. Pollen tubes were visualized by using transmitted confocal settings with a Pathway HT automated microscope (Atto Biosciences), using autofocus (20× objective). The rate was ≈15 sec per compound. Images were then viewed and scored for inhibition of pollen germination or alterations in pollen tube morphology as described. Of 2,016 compounds screened, 117 (5.8%) inhibited germination or altered tube morphology. The secondary screen bioactive compounds from the primary screen were diluted serially before addition to GM2 medium with tobacco pollen. The final dilutions were 10-, 100-, and 1000-fold. The pollen was from tobacco plants expressing GFP-RIP1; localization was detected with the Pathway HT, using GFP settings (20× objective). The autofocus routine captured a stack of five images (one image every 7 μm) to ensure images of GFP-RIP1 at pollen tube tips. The rate was approximately one compound per 45 sec. Of the 117 compounds examined, 16 displayed both inhibition of germination and mis-localization of GFP-RIP1 (0.8% of total). The phenotypes induced by these chemicals were examined at higher resolution with a SP2 LCSM (Leica). Of the 16 chemicals examined, several were judged to result in consistent mislocalization of RIP1-GFP and abnormal tip growth, including ES1 (prieurianin; Spectrum, catalog no. 00100068), the isothiocyanate erysolin (Spectrum, catalog no. 01501193), and the known phosphatase inhibitor cantheridin (Spectrum, catalog no. 01500814). The purity of ES1 was confirmed by LC/MS/MS at the Chemistry Instrumentation Facility at the University of California, Riverside. The on-line chemical database ChemMine (43) (http://bioweb.ucr.edu/ChemMineV2) was used for structural similarity searches to identify substructures and analogs. ES1 and limonoids were available from Spectrum.

Seedling Growth and Gravitropism Studies. *A. thaliana* ecotype Columbia (Col-0) was used in all experiments. Seeds were sterilized and sown on 0.5× MS medium (Invitrogen) containing 0.8% Phytoagar (Invitrogen) and vernalized for 48 h at 4°C, then grown in an 18-h light cycle at 22°C. For gravitropism, 4-day-old seedlings were rotated 90° and imaged after 24 h. For dark-grown seedlings, seeds were exposed to fluorescent white light (200 $\mu M \cdot m^{-2} \cdot s^{-1}$) for 4 h to induce germination, then kept in the dark for the times indicated. DR5-GUS assays for auxin activity were as described in ref. 44.

Chemical Treatments. Four-day-old light-grown seedlings were treated with ES1, Brefeldin A (BFA) (Sigma), naphthalene-1-acetic acid (NAA) (Sigma), or brassinolide (BL) (Wako Biochemistry) at the final concentrations indicated. Seedlings were transferred to 0.5× liquid MS medium, to which chemicals were added to the concentrations indicated. Stocks were 1 mM ES1, 17.8 mM BFA, 500 μM NAA, 100 μM BL, and 5 mM cycloheximide in 100% DMSO. FM4-64 was added to a concentration of 4 μM as indicated from a 10 mM stock in water. All microscopy used an SP2 LSCM (Leica) equipped with argon and HeNe lasers. Excitation was at 442 nm (CPF), 488 nm (GFP, FM4-64), and 543 nm (YFP). Detection of fluorescence used manufacturer settings where CFP and FM4-64 were coded red and GFP and YFP were coded green. GFP/CFP experiments were done by using sequential scanning.

Mutants and Construction of Marker Lines. Seeds for *bri1-116* were a gift from J.C.. Transgenic lines expressing SYP22-YFP and SYP61-CFP were constructed by using their native promoters according to Tian *et al.* (45), using the primers below. For both genes, YFP or CFP were placed at the N-terminal end of the fusion.

SYP22. P1 5′-GCT CGA TCC ACC TAG GCT TAC GTG TAA CCG TCG GGA TT-3′; P2 5′CAC AGC TCC ACC TCC ACC TCC AGG CCG GCC CAT CTT CTT CGC GAA ACC TCT TTT TT-3′; P3 5′ TGC TGG TGC TGC TGC GGC CGC TGG GGC CAT GAG TTT TCA AGA TTT AGA ATC AGG AAG-3′; P4 5′-CG TAG CGA GAC CAC AGG ATC TTT GTG ACA CTC ATT GAG CAA A-3′.

SYP61. P1 5′-GCT CGA TCC ACC TAG GCT TAA GGA TGT GCG TCA CAG GA-3′; P2 5′-TCC ACC TCC ACC TCC AGG CCG GCC CAT CCC GAA ATC AAC AAA ATT TTG C-3′; P3 5′-TGG TGC TGC TGC GGC CGC TGG GGC CAT GTC TTC AGC TCA AGA TCC ATT C-3′; P4 5′-CGT AGC GAG ACC ACA GGA TTA CGT TGG GCC TTA TCA GC-3′.

For the generation of the 35S promoter-driven YFP-SYP21 construct, the following primers were used: SYP21, 5′-TGG TGC TGC TGC GGC CGC TGG GGC ATG AGT TTC CAA GATC TCG AAG-3′ (forward) and 5′-CGA GCT CTT AGA CCA AGA CAA CGA TGA TA-3′ (reverse). The cYFP was amplified with the following primers: YFP 5′-GCT CTA GAG GCC GGC CTA TGG GAG GTG GAG GTG GAG CT-3′ and 5′-GGC CCC AGC GGC CGC AGC AGC ACC AGC CTT GTA CAG CTC GTC CAT GCC-3′ (reverse). A double template product was generated by using the two templates and YFP F and SYP21 R primers. The PCR product was digested with XbaI–SacI and ligated into the XbaI–SacI site of pCambia 1300. To amplify *RIP1* from an *Arabidopsis* flower cDNA library, the following gene-specific PCR primers were used: 5′RIP1-Bgl11, 5′-CCA GAT CTA TGC CAA GAC CAA GAG TT-3′) and 3;RIP1-KpnI, 5′-GCG GTA CCT CAC TTT TGC CCT TTC TTC CT-3′. Amplified *RIP1* fragments were ligated into pGEM T-EASY (Promega) to create *pGEM:RIP1*. To create *LAT52:GFP-RIP1* constructs, *RIP1* was removed from *pGEM:RIP1* with Bgl11/KpnI digestion and cloned into *pC1300LAT52:GFP* to create the translational fusion *LAT52:GFP-RIP1.* T2 transgenic tobacco plants (Samsun) were produced at the Plant Transformation Center at University of California, Riverside.

Quantitative PCR. Four-day-old seedlings were treated with BL, NAA, NAA plus BL, or an equivalent concentration of DMSO as indicated then frozen in liquid nitrogen. RNA was purified (Qiagen), and first-strand cDNA was synthesized (Invitrogen). For quantitative PCRs, SYBRGreen Supermix (BioRad) was used in reaction volume of 25 μl. Reactions were run on an iQ5 thermocycler (BioRad). Primers for gene-specific detection of BL-responsive NAC transcription factor (At5g46590) were 5′-GTT TAC CTC CAG GGT TCC GGT T-3′ (forward) and 5′-GCA CTG AGA TGC GAC ATC TTG G-3′ (reverse). Ubiquitin primers were 5′-GAT CTT TGC CGG AAA ACA ATT GGA GGA TGG T-3′ (forward) and 5′-CGA CTT GTC ATT AGA AAG AAA GAG ATA ACA GG-3′ (reverse). For relative quantification, ratios were calculated according to the method of Pfaffl (46). All C_t values were the average of three replicates and all treatments were subject to three biological replicates.

ACKNOWLEDGMENTS. We thank Drs. Lorena Norambuena, Kian Hematy, and Jirí Friml for helpful comments and discussion and Drs. David Carter and Thomas Girke at the Center for Plant Cell Biology for assistance with microscopy and bioinformatics, respectively. This work was supported by National Science Foundation Grants 2010-0520325 and MCB-0515963.

1. Cole RA, Fowler JE (2006) Polarized growth: Maintaining focus on the tip. *Curr Opin Plant Biol* 9:579–588.
2. Lavy M, *et al.* (2007) A Novel ROP/RAC effector links cell polarity, root-meristem maintenance, and vesicle trafficking. *Curr Biol* 17:947–952.
3. Molendijk AJ, Ruperti B, Palme K (2004) Small GTPases in vesicle trafficking. *Curr Opin Plant Biol* 7:694–700.
4. Yang Z, Fu Y (2007) ROP/RAC GTPase signaling. *Curr Opin Plant Biol* 10:490–494.
5. Gruenberg J (2001) The endocytic pathway: A mosaic of domains. *Nat Rev Mol Cell Biol* 2:721–730.
6. Ueda T, Yamaguchi M, Uchimiya H, Nakano A (2001) Ara6, a plant-unique novel type Rab GTPase, functions in the endocytic pathway of Arabidopsis thaliana. *EMBO J* 20:4730–4741.
7. Murphy AS, Bandyopadhyay A, Holstein SE, Peer WA (2005) Endocytotic cycling of PM proteins. *Annu Rev Plant Biol* 56:221–251.
8. Geldner N, Jurgens G (2006) Endocytosis in signalling and development. *Curr Opin Plant Biol* 9:589–594.
9. Dettmer J, Hong-Hermesdorf A, Stierhof YD, Schumacher K (2006) Vacuolar H+-ATPase activity is required for endocytic and secretory trafficking in Arabidopsis. *Plant Cell* 18:715–730.
10. Jaillais Y, Fobis-Loisy I, Miege C, Gaude T (2007) Evidence for a sorting endosome in Arabidopsis root cells. *Plant J* 53:237–247.
11. Jaillais Y, *et al.* (2007) The retromer protein VPS29 links cell polarity and organ initiation in plants. *Cell* 130:1057–1070.
12. Jurgens G, Geldner N (2007) The high road and the low road: Trafficking choices in plants. *Cell* 130:977–979.
13. Raikhel N, Hicks G (2007) Signaling from plant endosomes: Compartments with something to say! *Genes Dev* 21:1578–1580.
14. Gonzalez-Gaitan M (2003) Signal dispersal and transduction through the endocytic pathway. *Nat Rev Mol Cell Biol* 4:213–224.
15. Vert G, Nemhauser JL, Geldner N, Hong F, Chory J (2005) Molecular mechanisms of steroid hormone signaling in plants. *Annu Rev Cell Dev Biol* 21:177–201.
16. Geldner N, Hyman DL, Wang X, Schumacher K, Chory J (2007) Endosomal signaling of plant steroid receptor kinase BRI1. *Genes Dev* 21:1598–1602.
17. Richter S, *et al.* (2007) Functional diversification of closely related ARF-GEFs in protein secretion and recycling. *Nature* 448:488–492.
18. Teh OK, Moore I (2007) An ARF-GEF acting at the Golgi and in selective endocytosis in polarized plant cells. *Nature* 448:493–496.
19. Geldner N, *et al.* (2003) The Arabidopsis GNOM ARF-GEF mediates endosomal recycling, auxin transport, and auxin-dependent plant growth. *Cell* 112:219–230.
20. Grebe M, *et al.* (2003) Arabidopsis sterol endocytosis involves actin-mediated trafficking via ARA6-positive early endosomes. *Curr Biol* 13:1378–1387.
21. Michniewicz M, *et al.* (2007) Antagonistic regulation of PIN phosphorylation by PP2A and PINOID directs auxin flux. *Cell* 130:1044–1056.
22. Koul O, Daniewski WM, Multani JS, Gumulka M, Singh G (2003) Antifeedant effects of the limonoids from Entandrophragma candolei (Meliaceae) on the gram pod borer, Helicoverpa armigera (Lepidoptera: Noctuidae). *J Agric Food Chem* 51:7271–7275.

23. Sarker SD, Savchenko T, Whiting P, Sik V, Dinan L (1997) Two limonoids from Turraea obtusifolia (Meliaceae), prieurianin and rohitukin, antagonise 20-hydroxyecdysone action in a Drosophila cell line. *Arch Insect Biochem Physiol* 35:211–217.
24. Li J, Chory J (1997) A putative leucine-rich repeat receptor kinase involved in brassinosteroid signal transduction. *Cell* 90:929–938.
25. Xu J, Scheres B (2005) Dissection of Arabidopsis ADP-RIBOSYLATION FACTOR 1 function in epidermal cell polarity. *Plant Cell* 17:525–536.
26. Swarup R, *et al.* (2004) Structure-function analysis of the presumptive Arabidopsis auxin permease AUX1. *Plant Cell* 16:3069–3083.
27. Benkova E, *et al.* (2003) Local, efflux-dependent auxin gradients as a common module for plant organ formation. *Cell* 115:591–602.
28. Blakeslee JJ, *et al.* (2007) Interactions among PIN-FORMED and P-glycoprotein auxin transporters in Arabidopsis. *Plant Cell* 19:131–147.
29. Kleine-Vehn J, Dhonukshe P, Swarup R, Bennett M, Friml J (2006) Subcellular trafficking of the Arabidopsis auxin influx carrier AUX1 uses a novel pathway distinct from PIN1. *Plant Cell* 18:3171–3181.
30. Friml J, Palme K (2002) Polar auxin transport–old questions and new concepts? *Plant Mol Biol* 49:273–284.
31. Muller A, *et al.* (1998) AtPIN2 defines a locus of Arabidopsis for root gravitropism control. *EMBO J* 17:6903–6911.
32. Wisniewska J, *et al.* (2006) Polar PIN localization directs auxin flow in plants. *Science* 312:883.
33. Cutler SR, Ehrhardt DW, Griffitts JS, Somerville CR (2000) Random GFP::cDNA fusions enable visualization of subcellular structures in cells of Arabidopsis at a high frequency. *Proc Natl Acad Sci USA* 97:3718–3723.
34. Boevink P, *et al.* (1998) Stacks on tracks: The plant Golgi apparatus traffics on an actin/ER network. *Plant J* 15:441–447.
35. Nebenfuhr A, *et al.* (1999) Stop-and-go movements of plant Golgi stacks are mediated by the acto-myosin system. *Plant Physiol* 121:1127–1142.
36. Jaillais Y, Fobis-Loisy I, Miege C, Rollin C, Gaude T (2006) AtSNX1 defines an endosome for auxin-carrier trafficking in Arabidopsis. *Nature* 443:106–109.
37. Takano J, Miwa K, Yuan L, von Wiren N, Fujiwara T (2005) Endocytosis and degradation of BOR1, a boron transporter of Arabidopsis thaliana, regulated by boron availability. *Proc Natl Acad Sci USA* 102:12276–12281.
38. Robert S, *et al.* (2005) An Arabidopsis endo-1,4-beta-D-glucanase involved in cellulose synthesis undergoes regulated intracellular cycling. *Plant Cell* 17:3378–3389.
39. Sanderfoot AA, Kovaleva V, Bassham DC, Raikhel NV (2001) Interaction between synthaxins identify at least five SNARE complexes within the Golgi, prevacuolar system of Arabidopsis cells. *Mol Biol Cell* 12:3733–3743.
40. Paciorek T, *et al.* (2005) Auxin inhibits endocytosis and promotes its own efflux from cells. *Nature* 435:1251–1256.
41. Geldner N, Friml J, Stierhof YD, Jurgens G, Palme K (2001) Auxin transport inhibitors block PIN1 cycling and vesicle trafficking. *Nature* 413:425–428.
42. Nemhauser JL, Hong F, Chory J (2006) Different plant hormones regulate similar processes through largely nonoverlapping transcriptional responses. *Cell* 126:467–475.
43. Girke T, Cheng LC, Raikhel N (2005) A compound mining database for chemical genomics. *Plant Physiol* 138:573–577.
44. Surpin M, *et al.* (2005) The power of chemical genomics to study the link between endomembrane system components and the gravitropic response. *Proc Natl Acad Sci USA* 102:4902–4907.
45. Tian GW, *et al.* (2004) High-throughput fluorescent tagging of full-length Arabidopsis gene products in planta. *Plant Physiol* 135:25–38.
46. Pfaffl MW (2001) A new mathematical model for relative quantification in real-time RT-PCR. *Nucleic Acids Res* 29:e45.